J. A. Paivanas

Stationary Temperature Profiles and Heat Flux Distribution in a Plastic-encapsulated Circuit Package

Abstract: Thermal characteristics that are important to structural integrity are analyzed herein for a TTL, plastic-encapsulated package. By assuming that total module heat during operation is engendered at idealized junctions between lead wires and the chip surface, an analysis of its dissipation has been undertaken to determine internal steady-state temperature profiles and heat flux distribution. Based on junction heat sources of equal strength and on certain adiabatic assumptions, the multi-wire package has been modeled as a single-wire "composite" incorporating postulated heat dissipation mechanisms in representative plastic-to-wire and chip-to-lead frame thermal circuits. These circuits are treated, respectively, by axisymmetric and one-dimensional analyses. Instead of a partial differential equation approach in the former treatment, a less complicated method is devised which leads to characterization by a pair of linear ordinary differential equations. Their closed-form solution gives expressions for calculating two-dimensional temperature profiles and heat flux fractions. The resultant analyses are applied to a module containing 14 lead wires and operating at a given power level. The plastic and wire temperature profiles are seen to be nonlinear in the neighborhood of the chip surface and to coalesce axially into a common, essentially linear form in the outlying regions of the module. Constituent heat fluxes are also calculated for each thermal circuit, and some implications of the overall results to thermal stress are qualitatively discussed.

Introduction

The mechanical design of a semiconductor package must provide protection of the chip from a hostile ambient environment, a structurally reliable means for electrically connecting it to some external circuitry, and proper thermal dissipation of the heat generated during operation. In a TTL (transistor-transistor-logic) module of DIP (dual-inline-plastic) design, the main lead frame structure with attached chip and internal wiring is encapsulated in a molded plastic material as illustrated in Fig. 1. This design requires the plastic to be highly resistive to penetration by outside elements, to lend mechanical strength to the package, and to permit effective transfer of heat generated at the chip.

From a thermal standpoint, the latter two design characteristics are interdependent; hence the thermal compatibility of the various materials in the particular design configuration is of prime importance. In addition to different thermal coefficients of expansion, heat dissipation in the device is reflected by the coexistence of dissimilar temperature profiles in the lead wires, plastic, and the other constituent materials. These differences, in some combination, may result in inordinately high thermal stresses that could substantially reduce the operating life of the device. A particularly sensitive structural area is represented by the fine, plastic-encapsulated lead wires connecting the chip to the lead frame stations. In one version of the DIP design, thermal stress mitigation is approached by the use of a soft conformal coating material. applied prior to the plastic. This coating, located in the higher temperature region of the device, is primarily intended to act as a mechanical buffer between the rigid material of the plastic body and the lead wires. The other version of this design, however, does not use the conformal coating. Consequently, the thermal stress problem is augmented since the fine wires are totally encapsulated by rigid plastic.

Apart from a consideration of the expansion coefficient differences, one requirement for any assessment of the causes of thermal stress is a knowledge of steady-state temperature and heat flux distributions in the package. This poses a complex problem in analysis since the heat originating at the chip is dissipated simultaneously through the plastic, lead wires, and other constituent materials. A further complication is created by the irregular geometry of the device structure. Experimental studies have produced information relative to stationary wire-to-chip junction temperatures and outer surface temperatures as a function of heat dissipation level. However, due to prohibitively small dimensions and other configurational difficulties, experimental means cannot provide the further information on thermal characteristics that is needed in the assessment of the design. Consequently, the present study was undertaken to develop some mathematical insight into the character of the

steady-state temperature profiles and heat flux distribution in the rigid type of module.

This paper presents a theoretical analysis of the steady-state thermal characteristics of the TTL, DIP device containing rigid plastic as the sole encapsulating medium. It is based on a postulated model that assumes the total module heat to be generated by discrete heat source regions of equal strength, representing the aggregate effect of the actual lead wire-to-chip surface junction regions. The following sections give the underlying assumptions and rationale involved in the establishment of the model and its analysis. The resultant development provides a general means for calculating, in closed form, the temperature profiles in the wires and plastic as well as the constituent heat fluxes in these and certain other members of the package. It is applied to a particular package configuration containing fourteen lead wires and operating at a given power level.

Analysis

With reference to the module schematic shown in Fig. 1, the basic mathematical model describes two main thermal circuits through which the generated heat is concurrently dissipated. In one circuit a part of the heat, emanating from the wire junction regions at the chip surface, flows by conduction through a parallel arrangement of plastic and wires to the outer surface where it is transferred away by convection. In the second circuit, the other part of the generated heat is conducted through the chip thickness and lead frame to the outer convection surface. As shown in Fig. 2, the wire-to-chip junction regions are assumed to be represented by idealized, circular heat sources of equal strength. These mathematical sources are represented as disks embedded in a thin layer of the chip surface, from which heat is emitted in both radial and axial directions. The total heat generated in the module is assumed to be concentrated in this layer, from which the heat flows from both its upper and lower surfaces in an axial direction. As illustrated in Fig. 2, the normal heat flux per unit area (flux density) is predominant and uniform over the heat source areas, and decays to a relatively low level in the adjoining regions of the chip layer. It is further assumed that the chip layer is divided by a parallel surface, which acts as a thermal isolation partition between the two main thermal circuits. It divides the total heat generated into two main parts that are dissipated as described above, and is thus an adiabatic surface for each circuit considered separately. The thickness ϵ of the layer is assumed to be very small relative to the thickness of the chip and plastic. Consequently the location of the adiabatic partition is taken to be coincidental with the chip surface. The following analysis assumes constant thermal properties for the constituent materials with respect to temperature.

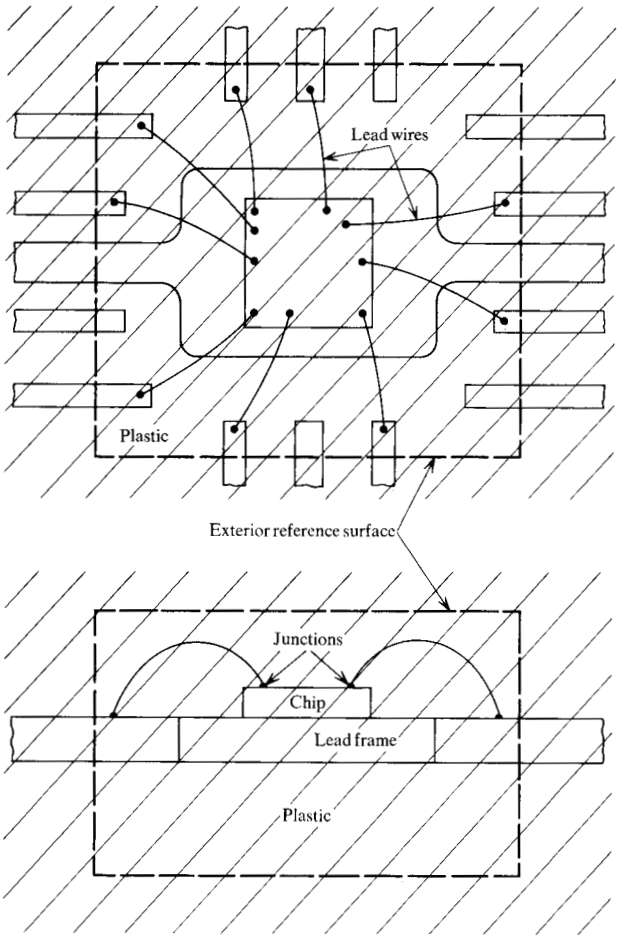

Figure 1 Schematic of TTL, DIP module.

Figure 2 Heat source model.

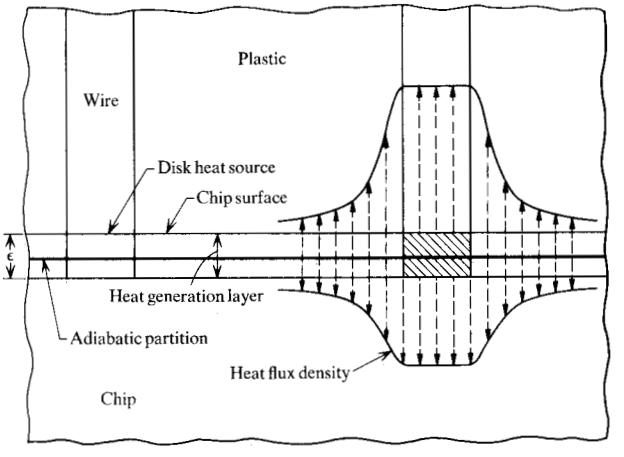

• *Plastic-wire model*

In view of the small geometric extent of the wires relative to the encapsulating plastic (see Fig. 1), the analytical structure of this thermal circuit can be pictured as in Fig. 3(a). The lead wires of length h and diameter d_w are

taken to be straight rods extending from the chip to the exterior surface. The heat sources, also of diameter d_w and located at the chip surface $x = 0$, collectively generate a quantity of heat denoted by q_{ts}, where the subscript s denotes the number of sources present. Of this amount, a quantity q_s flows through this thermal circuit while the remaining amount, denoted by Q_s, is conducted through the chip-lead frame circuit. The quantity q_s is transferred through the circuit in both the axial and transverse directions, due to the continuous heat exchange between the wire surfaces and adjoining plastic. Now, in view of the relatively large amount of plastic present, it can be assumed that q_s comprises a number of equal parts, corresponding to the number of lead wires. That is, each wire with its own given amount of plastic encapsulant is assumed to be associated with the dissipation of its own fraction of q_s. These heat flux fractions are individually associated with unequal amounts of plastic because of the asymmetry of the package design. However, because the smallest amount is still very large relative to a wire size, it is further assumed that the differences in quantity of plastic represent a small influence in creating differences among the thermal characteristics of the individual wire-plastic constituents of the package. Consequently, as described below, an "average" approach is taken in the model, in that equal heat flux fractions of q_s are assumed and these are associated with equal quantities of plastic having the same shape. The interpretation is thus that the thermal characteristics of each wire and its associated plastic are representative of the average of those existing in the actual package.

According to these assumptions, the corresponding temperature T_w of a wire at a given distance x from the chip surface is taken to be the same for all wires. Also, T_w is assumed to be constant over the cross-sectional area of a given wire, in view of its small diameter.

The transverse temperature profile in this thermal circuit, at a given location x, is assumed to have the form illustrated in Fig. 3(a). This assumption is based on two considerations. First, the cylindrical heat transfer surface of each wire is very small in comparison to parallel, concentric "surfaces" at remote radial locations in the surrounding plastic. The standard solution for steady, radial, conduction heat flow between coaxial cylindrical surfaces bounding a constant thermal conductivity material [1] indicates a temperature profile that decays logarithmically with radial distance from the heat source surface, its gradient varying inversely with radial location [2]. Accordingly, as illustrated in Fig. 3(a), the temperature gradient is highest at the wire surface $d = d_w$, where the temperature is T_w, and decreases with radial location d in the plastic to a smaller value at an arbitrary reference location d_r, where the temperature of the concentric surface area is denoted by T_r. In practice, d_r is typically much greater than d_w, and it follows that the temperature gradient at d_r will be very small relative to that at d_w. In fact, considering the range of operating values that $T_w - T_r$ might have, we may reasonably expect that the gradient at d_r will be of the order of zero. The second consideration pertains to the presence of multiple lead wires having the thermal characteristics described above. Their concurrent radial heat flows are, in a sense, opposed to one another, resulting in an interaction mechanism that tends to further decrease the already small radial temperature gradients. This interaction is manifest as an average effect over the total plastic in the package because of the asymmetric spacing of the wires. We thus assume for the plastic a temperature profile whose radial gradient decreases from a high value at the wire wall to zero at some remote radial location in the plastic. Due to the asymmetric configuration of the package, the zero value of the gradient occurs at different radial locations, depending on axial distance x from the chip surface and on the particular wire. On the other hand, because of the small size of the wires relative to the plastic, the effects of asymmetry tend to be overshadowed and it is reasonable to assume that these radial locations will also be essentially the same over the length of a given wire. Accordingly, it follows that the concentric cylindrical surface containing these points is adiabatic, since the radial temperature profiles are normal to it. Thus, each wire is assumed to be encased by a concentric plastic cylinder, having an adiabatic lateral surface and a diameter much larger than that of the wire [Fig. 3(a)]. The equal heat flux constituents of q_s are associated with equal quantities of plastic in accordance with the averaging assumption. Hence, the model of this thermal circuit is considered to be a set of s identical cylindrical plastic-wire "composites," each exerting the same fractional influence on the overall thermal characteristics of the circuit.

The analytic model is represented by the single-wire composite shown in Fig. 3(b). The diameter of the adiabatic plastic surface is denoted by d_p; the temperature of the plastic on this surface, at a location x, is denoted by T_p; the subscripts 0 and h refer, respectively, to specific values at the chip and exterior surfaces; and the partition area at the chip surface is adiabatic in accordance with the previous discussion. With reference to the definition of q_s, the steady-state heat flow q in the composite is given by

$$q \approx q_s/s \,. \tag{1}$$

The dissipation of q from the chip to the exterior surface involves internal heat transfer in both the radial and axial directions. Instead of using a partial differential equation approach, however, the analysis is performed as follows.

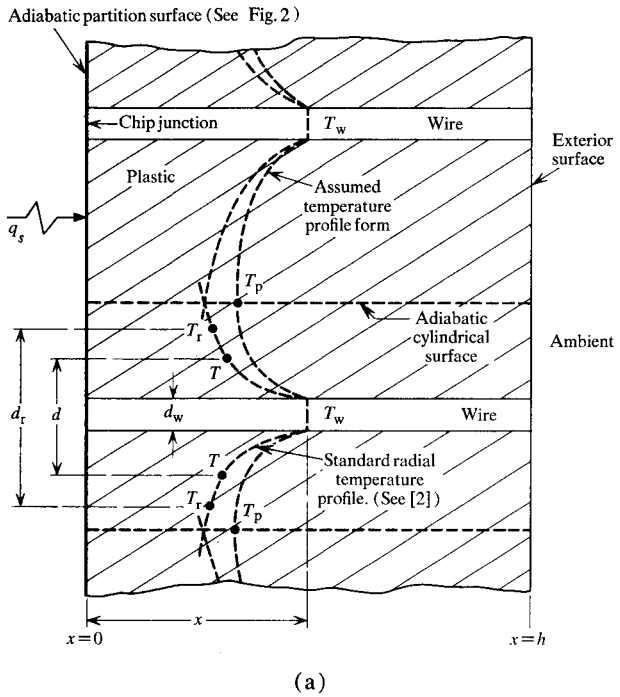

(a)

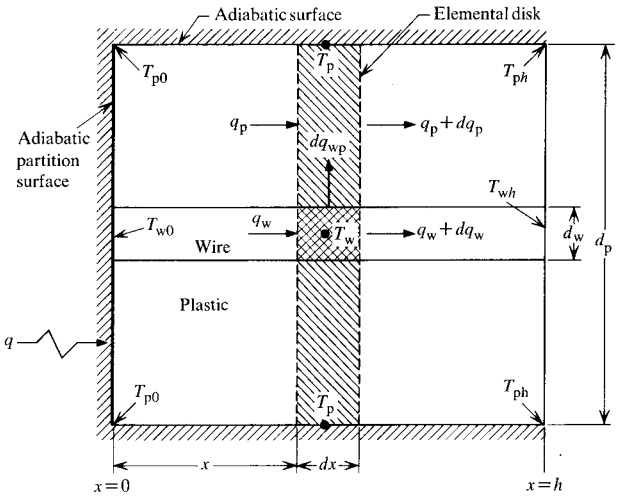

(b)

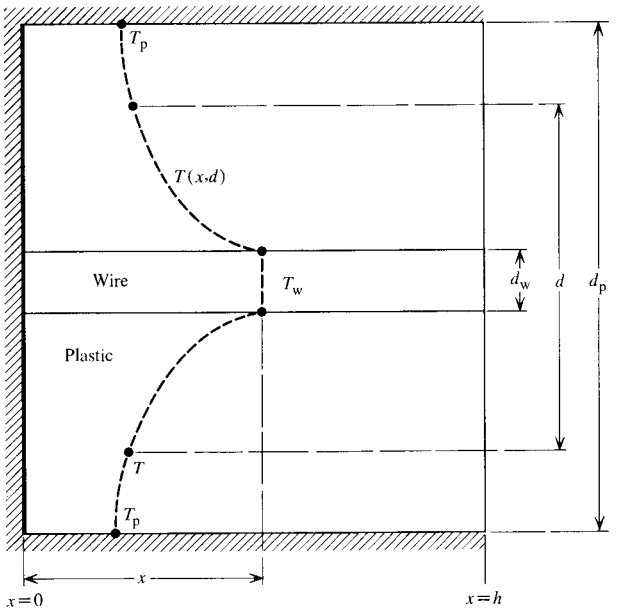

(c)

Figure 3 (a) Plastic-wire thermal circuit model; (b) single-wire composite model for heat transfer analysis; (c) assumption of radial temperature profile in plastic.

Referring to Fig. 3(b), we derive the constituent differential heat transfer expressions by considering an elemental disk at x, of diameter d_p and thickness dx. For conduction in the wire element, we have [1]

$$q_w = -k_w A_w \frac{dT_w}{dx}; \tag{2}$$

$$dq_w = -k_w A_w \frac{d^2 T_w}{dx^2}\, dx, \tag{3}$$

where q_w, k_w and A_w are the entering heat transfer rate, the thermal conductivity and the cross-sectional area of the wire, respectively. Equation (3) expresses the variation in q_w over dx due to radial conduction heat transfer dq_{wp} from the surface of the wire element to the plastic. Denoting the plastic thermal conductivity by k_p, we write for the cylindrical element [1]

$$dq_{wp} = Pk_p(T_w - T_p)dx, \qquad \text{where } P = \frac{2\pi}{\ln(d_p/dw)}. \tag{4}$$

For the axial conduction expressions in the plastic element, we refer also to Fig. 3(c), which shows the assumed form of the radial temperature profile. The profile $T(x,d)$ is a function of both x and d and is normal to the outer surface, in accordance with the adiabatic condition. The radial mean temperature T_m, at a location x, is given by

$$T_m = \frac{1}{(d_p - d_w)} \int_{d_w}^{d_p} T\, dd. \tag{5}$$

Therefore, the conduction expressions are

$$q_p = -k_p A_p \frac{dT_m}{dx}; \tag{6}$$

$$dq_p = -k_p A_p \frac{d^2 T_m}{dx^2}\, dx, \tag{7}$$

where A_p is the cross-sectional area of the plastic element. Equation (7) respresents the variation in q_p over dx, owing to the transfer of dq_{wp}. Next, a mathematical expression is assumed which qualitatively describes the

T profile form illustrated in Fig. 3(c). As implied before, the basis for this form is that it exhibits the geometric character of the standard temperature equation description [2] in the vicinity of the wire surface, which transforms with increase in radial location to a form having a zero gradient at $d = d_p$. Thus, the assumed T profile has a composite geometric character embodying both the above characteristics. The expression is given by

$$T = (T_w - T_p)\left(\frac{d_p - d}{d_p - d_w}\right)^n + T_p , \tag{8}$$

where n is a constant and, for any $n > 1$, the T profile is normal to the adiabatic wall [3]. The quantitative counterpart of the profile described by Eq. (8) is determined by the value of n, which is in turn determined by the appropriate boundary conditions as will be described below. Upon substitution of Eq. (8) into Eqs. (5), (6) and (7) we obtain, respectively,

$$T_m = \frac{nT_p + T_w}{n+1} ; \tag{9}$$

$$q_p = -\frac{k_p A_p}{n+1}\left(\frac{dT_w}{dx} + n\frac{dT_p}{dx}\right) ; \tag{10}$$

$$dq_p = -\frac{k_p A_p}{n+1}\left(\frac{d^2T_w}{dx^2} + n\frac{d^2T_p}{dx^2}\right) dx . \tag{11}$$

This completes the establishment of the constituent heat transfer expressions for the model.

The conditions for a heat balance in the elemental volume are

$$q_w = q_w + dq_w + dq_{wp} ; \tag{12}$$

and

$$q_p = q_p + dq_p - dq_{wp} , \tag{13}$$

for the wire and plastic, respectively. Substitution of Eqs. (3) and (4) into Eq. (12) results in

$$\frac{d^2T_w}{dx^2} = \frac{Pk_p}{A_w k_w}(T_w - T_p) . \tag{14}$$

Adding Eqs. (12) and (13) and substituting Eqs. (3) and (11) into the result gives

$$\frac{d^2T_p}{dx^2} = -\gamma\frac{d^2T_w}{dx^2} , \tag{15}$$

where

$$\gamma = \frac{1}{n}\left[1 + (n+1)\frac{k_w A_w}{k_p A_p}\right] . \tag{16}$$

We proceed next to obtain the temperature solutions of the ordinary differential equation system given by Eqs. (14) and (15). Integrating Eq. (15) twice gives

$$T_p = -\gamma(T_w + a_1 x + a_2) , \tag{17}$$

where a_1 and a_2 are constants of integration. Equation (17) expresses the relationship between the plastic and wire temperatures at a location x. To obtain the relationship between T_w and x, we substitute Eq. (17) into Eq. (14), resulting in

$$\frac{d^2T_w}{dx^2} - \alpha T_w - \beta(a_1 x + a_2) = 0 , \tag{18}$$

where

$$\alpha = (n+1)\frac{P}{A_p}\left(\frac{\gamma+1}{n\gamma-1}\right) \tag{19}$$

and

$$\beta = \left(\frac{\gamma}{\gamma+1}\right)\alpha . \tag{20}$$

The required relationship is obtained from the solution of Eq. (18), and is

$$T_w = a_3 \exp(\alpha^{1/2}x) + a_4 \exp(-\alpha^{1/2}x) - \frac{\beta}{\alpha}(a_1 x + a_2) , \tag{21}$$

where a_3 and a_4 are constants of integration. The general temperature solutions, represented by Eqs. (17) and (21), contain five constants, a_1, a_2, a_3, a_4 and n, which are determined by imposition of certain boundary conditions as follows.

The integration constants are determined from the following conditions:

$$T_w = T_{w0} , \; T_p = T_{p0} \quad \text{and} \quad q = q_{w0} + q_{p0} \text{ at } x = 0 ; \tag{22}$$

$$T_w = T_{wh} , \; T_p = T_{ph} \quad \text{and} \quad q = q_{wh} + q_{ph} \text{ at } x = h . \tag{23}$$

Because of the two adiabatic surfaces [Fig. 3(b)], the total heat influx at $x = 0$ is equal to the total efflux at $x = h$. This condition is indicated by the last equality in Eqs. (22) and (23). The first integration constant is determined by the use of either equality. Choosing the one in Eq. (22) and substituting Eqs. (2), (10) and (17), with the temperature derivatives referred to the $x = 0$ location, we obtain

$$a_1 = \left(\frac{n+1}{n}\right)\frac{q}{k_p A_p \gamma} . \tag{24}$$

Next, referring Eqs. (17) and (21) to $x = 0$ results in

$$a_2 = -\frac{T_{p0} + \gamma T_{w0}}{\gamma} ; \tag{25}$$

$$a_3 + a_4 = \frac{T_{w0} - T_{p0}}{\gamma + 1} . \tag{26}$$

Finally, from Eqs. (17) and (21) referred to $x = h$, in conjunction with Eqs. (24), (25) and (26), we obtain

$$a_3 = \frac{T_{wh} - T_{ph} - (T_{w0} - T_{p0})\exp(-\alpha^{1/2}h)}{(\gamma+1)[\exp(\alpha^{1/2}h) - \exp(-\alpha^{1/2}h)]} . \tag{27}$$

The exponent n of Eq. (8) is determined by the introduction of one other assumption, which states that the axial temperature gradient in the plastic is zero at $x=0$. Accordingly, with reference to Eq. (17), we write

$$\frac{1}{\gamma}\left(\frac{dT_p}{dx}\right)_{x=0} = -\left(\frac{dT_w}{dx}\right)_{x=0} - a_1 = 0, \tag{28}$$

where the subscript refers to the derivative value at the $x=0$ location. This assumption is justified on the grounds that the heat flux density is predominant at the heat source region on the chip surface (see Fig. 2). At $x=0$ and $d=d_w$, the axial temperature gradients of the wire and plastic are identical. As $d \to d_p$ along $x=0$, the gradient in the plastic decreases and tends toward zero, on account of the corresponding decrease of the heat flux density. Consequently, since $d_p \gg d_w$, it is reasonable to assume Eq. (28). Substitution of Eqs. (21), (24), (25) and (26) into (28) results in

$$a_3 = -\frac{1}{2(\gamma+1)}\left[\left(\frac{n+1}{n}\right)\frac{q}{k_p A_p \gamma \alpha^{1/2}} - (T_{w0} - T_{p0})\right], \tag{29}$$

where a_3 is given by Eq. (27). In addition there is one other relationship, which is obtained by referring Eq. (17) to $x=h$ and substituting Eqs. (24) and (25) into it. The result is

$$\left(\frac{n+1}{n}\right)\frac{qh}{k_p A_p} = \gamma(T_{w0} - T_{wh}) + T_{p0} - T_{ph}. \tag{30}$$

The exponent n and one boundary temperature can be obtained from Eqs. (29) and (30), where the other temperatures and indicated quantities are given. In the present application, we solve these equations for n and T_{p0} since for a given value of q, T_{w0}, T_{wh} and T_{ph} are known. This calculation is simplified by considering the order of magnitude of certain quantities. The exponent n in Eq. (8) is greater than one by definition and for $n \to \infty$, the parameters γ and α given by Eqs. (16) and (19) decrease and approach constant values. Furthermore, in view of the size of h and the magnitudes of γ and α in the interval $1 < n \leq \infty$, the quantity $\exp(\alpha^{1/2}h) \gg 1$ in Eq. (27). Also, for $T_{wh} \approx T_{ph}$ and in view of the expected range of $(T_{w0} - T_{p0})$, we conclude from Eq. (27) that $a_3 \approx 0$. Consequently, using Eqs. (16), (19), (29) and (30) with $a_3 = 0$, we obtain expressions for n and T_{p0} as follows:

$$n = \frac{1 + (k_w A_w / k_p A_p)}{\gamma - (k_w A_w / k_p A_p)}, \tag{31}$$

where γ is calculated from

$$\gamma^3 + \gamma^2 = \frac{A_w k_w}{P k_p}\left[\frac{k_p A_p}{q}\left(1 + \frac{k_w A_w}{k_p A_p}\right)(T_{w0} - T_{wh}) - h\right]^{-2}. \tag{32}$$

This cubic equation in γ has only one positive real root; the other two roots are not pertinent here since they are negative real or imaginary. Finally, the corresponding temperature T_{p0} is obtained most conveniently from Eq. (30), with the values of n and γ given by Eqs. (31) and (32).

With the determination of the five constants, the two-dimensional temperature field in the model composite for a given value of q can now be calculated by means of Eqs. (8), (17) and (21). The constituent influx fractions of q at $x=0$ are obtained from Eqs. (2), (10), (16) and (28), and are

$$\frac{q_{p0}}{q} = \frac{1}{n\gamma}; \tag{33}$$

$$\frac{q_{w0}}{q} = 1 - \frac{1}{n\gamma}. \tag{34}$$

The corresponding efflux fractions at $x=h$ are obtained from Eqs. (2), (10), (17) and (21), in conjunction with the condition that $T_{wh} = T_{ph}$. The results are

$$\frac{q_{ph}}{q} = \frac{1}{\gamma+1}\left(\frac{n+1}{n}\right); \tag{35}$$

$$\frac{q_{wh}}{q} = \frac{1}{\gamma+1}\left(\frac{n\gamma - 1}{n}\right). \tag{36}$$

• *Chip-lead frame model*

To determine the value of q in a given amount of module heat dissipation, we require a means for calculating the associated heat transfer in the chip-to-lead frame circuit. This circuit, as in the previous case, is also assumed to consist of s identical "composites" where the heat flux Q in each is given by

$$Q \approx Q_s/s. \tag{37}$$

The model for the chip-to-lead frame composite is illustrated in Fig. 4(a). The chip subdivision is taken to be a cylindrical extension of the plastic, also with an adiabatic lateral surface. The transfer of Q from the adiabatic partition at the chip surface to the lead-frame interface takes place one-dimensionally through the chip segment thickness t_c, and over an equivalent constant cross-sectional area A_{ce}, where $A_w < A_{ce} < A_p$. At the chip-lead frame interface, Q is assumed to split into two equal parts q_f which transfer one-dimensionally to the outer surface through the lead frame branches of length t_f and cross-sectional area A_f. The latter quantity represents $1/s$ of the total cross-sectional area of the lead frame. Because of the relatively high conductive capacity of the lead frame, it is assumed that any other heat transfer from its lateral surfaces through the plastic to the exterior surface is negligible. With reference to Fig. 4(a), we write

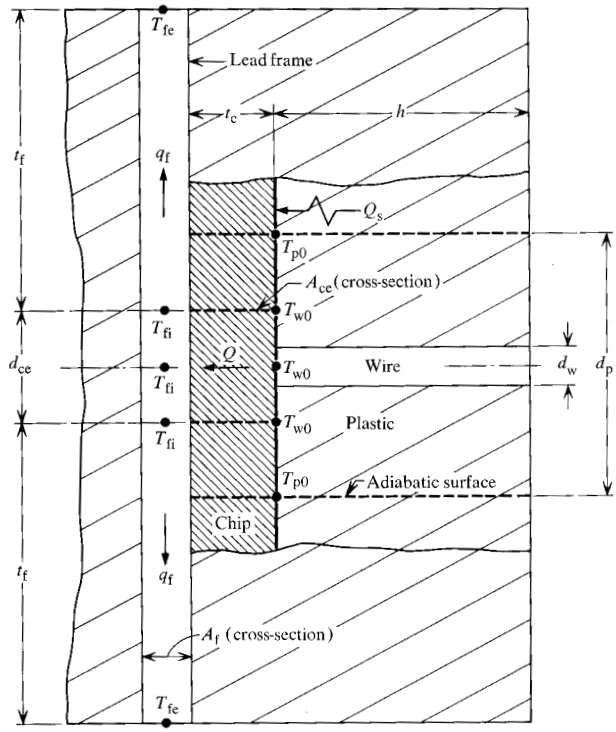

(a)

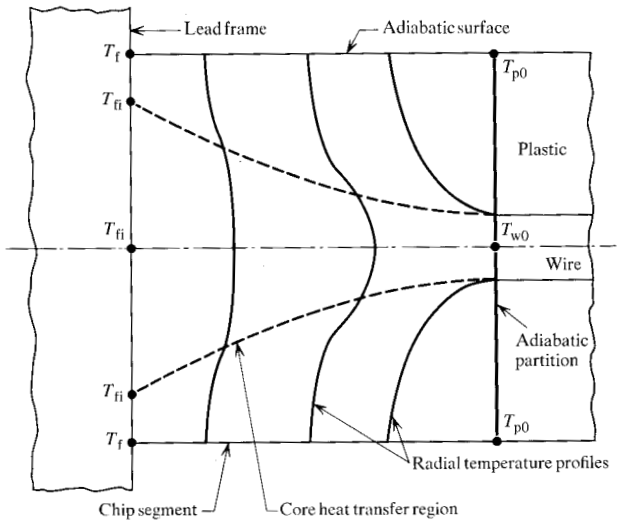

(b)

$Q = 2q_f$; whence (38)

$$Q = \frac{k_c A_{ce}}{t_c}(T_{w_0} - T_{fi}) = \frac{2k_f A_f}{t_f}(T_{fi} - T_{fe}) , \quad (39)$$

where k_c and k_f are the thermal conductivity of the chip and lead frame; T_{fi} and T_{fe} denote the uniform temperatures at the chip-lead frame interface region and the exterior-lead frame surface respectively; and T_{w_0} has been defined previously except that here it is constant over

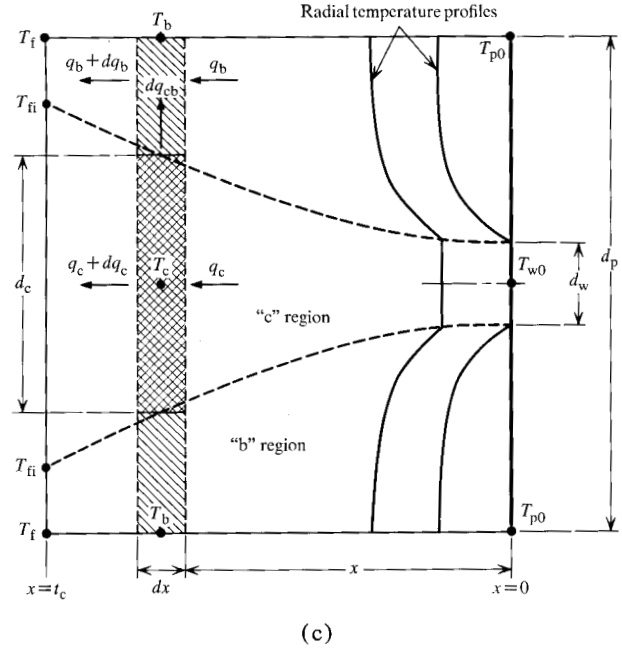

(c)

Figure 4 (a) Chip-lead frame thermal circuit model; (b) qualitative thermal characteristics in chip segment model; (c) chip segment heat transfer model.

A_{ce} at the chip surface. Eliminating T_{fi} in Eq. (39), we obtain

$$Q = \frac{T_{w_0} - T_{fe}}{(t_c/k_c A_{ce}) + (t_f/2k_f A_f)} , \quad (40)$$

for the heat flux in the chip-lead frame composite. From the definition of q_{ts}, the relationship of heat dissipation quantities in each pair of model composites is given by

$$q_t \approx q_{ts}/s = Q + q . \quad (41)$$

At this point, all quantities in Eq. (40) can be specified with the exception of A_{ce}, which is now determined as follows.

The actual conduction heat transfer mechanism in each cylindrical chip segment is taken to be two-dimensional with axial symmetry. As illustrated in Fig. 4(b), the radial temperature profiles are such that the bulk of the radial temperature drop occurs within a so-called "core" region. The cross-sectional area of this region increases with axial distance from the chip surface, due to the divergence of the heat flow streamlines. At the chip surface, its area is A_w, over which T_{w_0} is constant; at the chip-lead frame interface, its area is some value much larger than A_w, but less than A_p, and over which the temperature T_{fi} is constant. The larger part of Q occurs through the core region, as opposed to that occurring in the adjoining region, in accordance with the assumed characteristics of the transfer mechanism. It is possible, but considerably difficult, to obtain an analyt-

ical definition of the actual core shape and other parameters that would be required to ultimately determine Q. This difficulty is due to the mathematical nonlinearity introduced by the unknown variation of the core area. As it turns out, however, a complete analysis is not necessary; it is possible to justify an approximate means for conservatively estimating A_{ce}.

Figure 4(c), the assumed analytic model based on Fig. 4(b), shows a core, or "c" region, of variable diameter d_c and across which the temperature T_c is constant. In the adjoining, or "b" region, the radial temperature profiles decrease and are normal to the adiabatic cylindrical wall where the temperature is T_b. The temperature profiles in this region are assumed to have a mathematical form analogous to Eq. (8) where, in this instance, the exponent is denoted by m. For an elemental disk at x, of diameter d_p and thickness dx, the constituent element heat balance expressions are

$$q_c = q_c + dq_c + dq_{cb}\,; \tag{42}$$

$$q_b = q_b + dq_b - dq_{cb}\,, \tag{43}$$

where the constituent heat flux rates are as indicated in the figure. Proceeding in a manner analogous to that for the previous model, we write

$$q_c = -k_c A_c T_c'\,; \tag{44}$$

$$dq_c = -\left(A_c T_c'' + A_c' T_c'\right) k_c dx\,; \tag{45}$$

$$dq_{cb} = \frac{4\pi k_c}{\ln(A_b/A_c)}\,(T_c - T_b)\,dx\,; \tag{46}$$

$$q_b = -\left(\frac{k_c}{m+1}\right)(A_b - A_c)\,(T_c' + mT_c')\,; \tag{47}$$

and

$$dq_b = -\left(\frac{k_c}{m+1}\right)$$

$$\times\left[(A_b - A_c)(T_c'' + mT_b'') - A_c'(T_c' + mT_b')\right] dx\,, \tag{48}$$

where the single and double primes indicate first and second derivatives with respect to x; A_c and A_b are the cross-sectional areas of the elements; and k_c denotes the thermal conductivity of the chip. Upon substitution of Eqs. (44) through (48) into Eqs. (42) and (43), we obtain the following system of nonlinear differential equations:

$$A_c T_c'' + A_c' T_c' - \frac{4\pi(T_c - T_b)}{\ln(A_b/A_c)} = 0\,; \tag{49}$$

$$T_c''\left(A_c + \frac{A_b}{m}\right) + A_c'(T_c' - T_b') + (A_b - A_c)\,T_b'' = 0\,. \tag{50}$$

The area and temperature solutions of Eqs. (49) and (50) are difficult to obtain and are not sought here since we can establish, by considering their expected mathematical character, an approximate calculation of A_{ce}. Since the temperature solutions for this model will be basically exponential, the coupled area variation solution will also be nonlinear and describe a core boundary shape of the kind sketched in Fig. 4(c). Assuming that A_c at $x = t_c$ is equal to A_p, we consider the aggregate of heat flux in the "c" and "b" regions (i.e., Q) to take place in a "c" region having boundary areas A_p and A_w. The equivalent heat flow area A_{ce} depends on the unknown relationship between A_c and x; consequently we examine possible variations of this relationship in conjunction with the effect on Eq. (40) of the corresponding values of A_{ce}. Considering relationships ranging from a linear form to an extreme case of the illustrated form, and also noting that $A_p \gg A_w$, we conclude finally that a conservative estimate is given by the simple expression

$$A_{ce} \approx \frac{\pi d_{ce}^{\,2}}{4} = \frac{\pi}{4}\left(\frac{d_p + d_w}{2}\right)^2. \tag{51}$$

Application and discussion

The preceding analysis is applied to a particular module configuration containing $s = 14$ lead wires. The estimated values of the geometric and thermal conductivity parameters of the package are:

$d_w \approx 0.001$ in.;
$d_p \approx 0.08$ in.;
$h \approx 0.08$ in.;
$t_c \approx 0.008$ in.;
$t_f \approx h + \frac{1}{2}(d_p + d_w) \approx 0.10$ in.;
$k_w \approx 125$ btu/hr-ft-°F (gold);
$k_p \approx 0.315$ btu/hr-ft-°F;
$k_c \approx 50$ btu/hr-ft-°F; and
$k_f \approx 15$ btu/hr-ft-°F (standard type K Kovar).

The thermal conductivities represent average values taken over a considered operating temperature range of 180 to 260°F. The calculated cross-sectional areas are:

$A_w = 0.00545 \times 10^{-6}$ ft^2;
$A_p = 34.89 \times 10^{-6}$ ft^2;
$A_{ce} = 8.94 \times 10^{-6}$ ft^2 [from Eq. (51)]; and
$A_f = 0.185 \times 10^{-6}$ ft^2,

where A_f is based on lead frame cross-sectional dimensions of 0.015 in. thick by 0.025 in. wide.

For a module power operating level of 350 mW, corresponding to a total heat dissipation $q_{ts} = 1.194$ btu/hr, the following temperatures from reported experimental measurements are used:

$T_{w_0} \approx 251.7$°F, and
$T_{w_h} \approx T_{p_h} \approx T_{fe} \approx 208$°F (i.e., an isothermal exterior surface).

From Eqs. (41), (40), (32), (31), (19), (30) and (24) through (27), we obtain the following quantities.

$q_t \approx 0.085$ btu/hr ;
$Q \approx 0.030$ btu/hr ;
$q \approx 0.055$ btu/hr ;
$\gamma = 0.56$;
$n = 2.13$;
$\alpha = 1.032 \times 10^6$ ft^{-2} ;
$T_{p_0} = 239$°F ;
$a_1 = 13{,}132$;
$a_2 = -678$;
$a_3 = 0$; and
$a_4 = 8.28$.

The axial temperature profiles in the plastic and wire, calculated by Eqs. (17) and (21), respectively, are plotted in Fig. 5(a). The radial temperature profiles in the plastic, with constant axial location as a parameter, are calculated by Eq. (8) and plotted in Fig. 5(b). By Eqs. (33) through (36), the calculated constituent influx and efflux fractions of q are, respectively,

$$\frac{q_{p_0}}{q} = 0.838 \; ; \; \frac{q_{w_0}}{q} = 0.162 \text{ and}$$

$$\frac{q_{p_h}}{q} = 0.942 \; , \; \frac{q_{w_h}}{q} = 0.058 \; ,$$

from which $(q_{w_0} - q_{w_h})/q = 0.104$ is the fraction transferred radially from the wire to the plastic, over the interval $0 \leq x \leq h$. Furthermore, while the thermal conductivity of the plastic is much lower than that of the wire, its relative heat flux fraction at both locations is much higher, due to the comparatively small wire size (i.e., $A_w \ll A_p$) . On the other hand, in terms of heat flux fraction per unit area (flux density), viz.,

$$\frac{q_{p_0}}{qA_p} = 0.024 \times 10^6 \text{ ft}^{-2} \; ; \; \frac{q_{w_0}}{qA_w} = 29.72 \times 10^6 \text{ ft}^{-2} \text{ and}$$

$$\frac{q_{p_h}}{qA_p} = 0.027 \times 10^6 \text{ ft}^{-2} \; ; \; \frac{q_{w_h}}{qA_w} = 10.64 \times 10^6 \text{ ft}^{-2} \; ,$$

the reverse situation is true, according to the assumed heat generation mechanism in the chip surface layer (Fig. 2).

In operation of the module, the actual flux density of the generated heat tends to occur predominantly at the wire-to-chip junction regions. In the adjoining regions, the flux density is relatively nonuniform and much lower, and is due both to conduction transfer from the junctions and to contributions from other, relatively minor heat-generating sites. In view of this behavior, the present model is predicated on concentration of the total generated heat in the neighborhood of the chip surface. The concept of a heat generation layer has thus been postulated, in which all heat generation is lumped at the junction source regions, and in which the idealized normal flux density variation is as shown in Fig. 2.

The assumption of a particular form for radial temperature profiles in the plastic, such as $T(x,d)$ given by Eq. (8), implies a particular mathematical variation of this density in the chip layer region adjoining a heat source. For possible alternative forms of Eq. (8), satisfying the prescribed end conditions at $d = d_w$ and $d = d_p$ [Fig. 3(c)], correspondingly different flux density distributions exist. In fact, for the present problem it is interesting to note the possible existence of a unique form of Eq. (8), which would provide the same information as that from a partial differential equation approach. Such an expression would, of course, be very difficult to determine in closed form. In the present investigation, we have taken the less complicated approach of assuming Eq. (8) as a good approximation in view of the intrinsic character of the flux density decay. As shown in the analysis, its nonlinearity exponent n is uniquely determined for the particular boundary conditions imposed.

In the temperature profiles plotted in Figs. 5(a) and 5(b), a maximum junction-plastic temperature difference of $T_{w_0} - T_{p_0} = 12.7$°F is indicated at the chip surface $x/h = 0$. This difference decreases with increase in x/h , as the wire and plastic temperature profiles coalesce into a single, essentially linear form for $x/h > 0.4$. As seen by Eq. (28), the slope of the wire profile T_w' at $x = 0$ is equal to $-a_1$ and is thus very high, since $a_1 = 13{,}132$. Other calculations for the present case, at 200-mW and 500-mW power levels, have indicated the persistence of high a_1 values, 6847 and 17,937 respectively. Consequently, in a vanishingly small region around $x = 0$, a rapid decrease in T_w' is indicated, which in turn is associated with a state of high stress concentration. This situation is augmented here by the characteristics of the local radial temperature gradient in the adjoining plastic, as may be seen by obtaining the slope equation from Eq. (8)

$$\left(\frac{dT}{dd}\right)_{x=0,\, d=d_w} = -n \left(\frac{T_{w_0} - T_{p_0}}{d_p - d_w}\right) ,$$

pertaining to the junction location [3]. In practice, however, the effect of this stress concentration is mitigated to an extent by the connection joint between the wire and chip surface. Still, an unknown level of stress concentration remains, which increases nonlinearly with q, and which encroaches to some measure on the fatigue life of the device. Finally, for the chip surface vicinity in particular, the thermal stress level in the wire and plastic can be intensified due to the nature of the temperature profiles, in addition to the effect of the relatively higher expansivity of the plastic. These observations are qualitative, of course, since the scope of the present work

does not include a quantitative study of thermal stress as such. The package heat transfer characteristics shown here, however, do imply certain stress characteristics which should be considered in applications.

The degree to which the above characteristics are manifest is a function of the value of q associated with a given power operating level of the module. The present example indicates that approximately 65 percent of the generated heat q_t [Eq. (41)] is dissipated in the plastic-to-wire circuit (i.e., q), while the remaining 35 percent (i.e., Q) is transferred through the chip-to-lead frame circuit. The analysis of the latter circuit assumes, in effect, that the heat transfer through the chip body, Q_s, is conducted solely through the lead frame length, i.e., that any transfer occurring from the lateral surfaces, through the plastic, to the exterior surface is estimated to be relatively small. Referring to Eq. (40), we observe that the thermal resistance of the lead frame component, given by $R_f = t_f/2k_fA_f$, is inherently much higher than that of the chip segment, $R_c = t_c/k_cA_{ce}$. Consequently, the value of Q is influenced primarily by R_f and any means that can be applied to reduce the value of R_f will result in an increase in Q, with a corresponding decrease in q [Eq. (41)]. Finally, implicit in the present model is the assumption that the thermal resistance at the chip-to-lead frame interface is negligibly small because of the bonding process.

In any application of the present analysis certain geometric parameters must be estimated, since the actual configuration of the package is asymmetric. However, due to the large extent of the constituent materials relative to the fine wires and their junction regions, certain attendant thermal insensitivities exist that make it possible to obtain good estimates of these parameters. The determination of n [Eqs. (31) and (32)] for the prescribed boundary conditions was faciliated by an order-of-magnitude analysis indicating that $a_3 \approx 0$. For situations where $T_{wh} \neq T_{ph}$ (nonisothermal exterior surface) and where $\exp(\alpha^{1/2}h)$ is not much greater than 1, the magnitude of a_3 may not be of the order of zero; hence, n and T_{p0} must be calculated from Eqs. (29) and (30) for given values of the other parameters.

Summary

The present study concerns the influence of thermal dissipation behavior on the structural integrity of a TTL, DIP module design and provides a mathematical model for the calculation of steady-state thermal characteristics, corresponding to a given power operating level with associated junction and exterior surface temperatures. By postulating a kind of thermal symmetry, the asymmetric, multi-wire package is envisaged as consisting of s geometrically tractable, single-wire "composites," each representing the main thermal circuits in the device, and

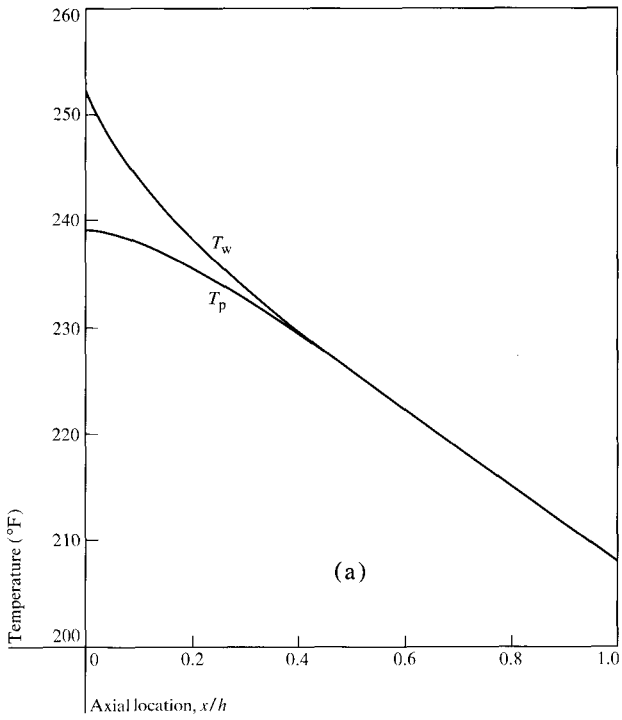

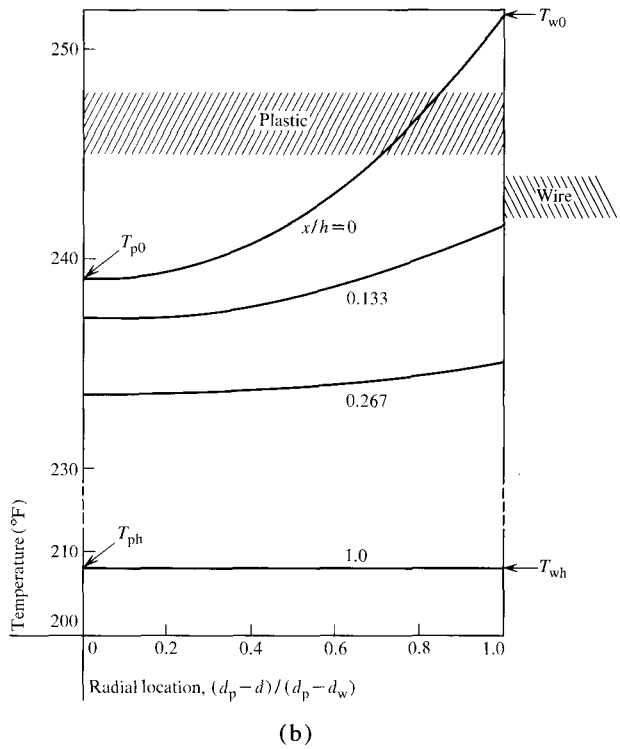

(b)

Figure 5 (a) Temperature vs axial location for wire and plastic, 350-mW module power level. (b) Temperature vs radial location for plastic, with axial location parametric and a 350-mW module power level.

each exerting the same fractional influence on its overall thermal characteristics. The analysis applies to a particular module design, incorporating rigid plastic encapsulation without the use of a conformal coating material, and has yielded closed-form expressions for the calculation of axisymmetric temperature profiles in the plastic-to-wire part of the model, as well as the heat flux distribution in this and the associated chip-to-lead frame. From its application to a package design containing 14 lead wires, certain qualitative inferences as to the thermal stress in the wires, plastic, and junction regions have been drawn from the predicted temperature profiles and heat flux distribution.

The actual module configuration inherently presents insurmountable difficulties in obtaining experimental measurements to support the thermal model. Apart from measurements of junction and exterior surface temperatures as a function of power level, detailed measurements of interior temperatures are precluded by the very small dimensions of the device. While experimental confirmation is not available, the present model nevertheless provides a means for obtaining an insight into the operating thermal mechanism in the package.

Acknowledgments

The author expresses his appreciation to M. S. Mansuria for providing helpful information on constructional features of the subject device, and to J. H. Kelly for his support in the preparation of this manuscript.

References and footnotes

1. M. Jakob, *Heat Transfer*, Volume I, John Wiley and Sons, Inc., New York 1956.
2. The equation for radial temperature distribution from the standard solution, and its corresponding slope equation are:

   $T = (T_w - T_r)[1n(d/d_r)/1n(d_w/d_r)] + T_r$; and

   $dT/dd = (1/d)[(T_w - T_r)/1n(d_w/d_r)]$.

3. The slope of the T profile given by Eq. (8),

   $dT/dd = -n\,(d_p - d)^{n-1}\,(T_w - T_p)/(d_p - d_w)^n$,

   is zero at $d = d_p$ for any value of $n > 1$.

Received July 16, 1971

The author is located at the IBM Components Division Laboratory, East Fishkill (Hopewell Junction), New York 12533.